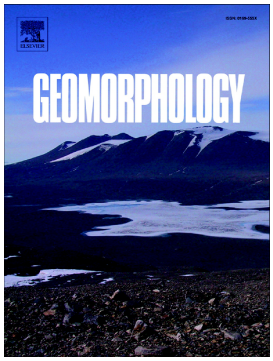

Ridge-like lava tube systems in southeast Tharsis, Mars

Jiannan Zhao, Jun Huang, Michael D. Kraft, Long Xiao, Yun Jiang

PII: S0169-555X(17)30327-6
DOI: doi: 10.1016/j.geomorph.2017.08.023
Reference: GEOMOR 6118

To appear in: *Geomorphology*

Received date: 15 March 2017
Revised date: 7 August 2017
Accepted date: 7 August 2017

Please cite this article as: Jiannan Zhao, Jun Huang, Michael D. Kraft, Long Xiao, Yun Jiang , Ridge-like lava tube systems in southeast Tharsis, Mars, *Geomorphology* (2017), doi: 10.1016/j.geomorph.2017.08.023

Ridge-like lava tube systems in southeast Tharsis, Mars

Jiannan Zhao[1,2], Jun Huang[1,2]*, Michael D. Kraft[3], Long Xiao[1], Yun Jiang[2]

[1] State Key Laboratory of Geological Processes and Mineral Resources, Planetary Science Institute, School of Earth Sciences, China University of Geosciences, Wuhan 430074, China.

[2] Key Laboratory of Planetary Sciences, Chinese Academy of Sciences, Nanjing 210008, China.

[3] Geology Department, Western Washington University, Bellingham, WA 98225, USA.

***Corresponding author: Jun Huang (junhuang@cug.edu.cn)**

Abstract

Lava tubes are widely distributed in volcanic fields on a planetary surface and they are important means of lava transportation. We have identified 38 sinuous ridges with a lava-tube origin in southeast Tharsis. The lengths vary between ~14 and ~740 km, and most of them occur in areas with slopes <0.3°. We analyzed their geomorphology in detail with CTX (Context Camera) and HiRISE (High Resolution Imaging Science Experiment) images and DTM (digital terrain model) derived from them. We identified three cross-sectional shapes of these sinuous ridges: round-crested, double-ridged, and flat-crested and described features associated with the lava tubes, including branches, axial cracks, collapsed pits, breakout lobes, and tube-fed lava deltas. Age determination results showed that most of the lava tubes formed in Late Hesperian and were active until the Hesperian-Amazonian boundary. We proposed that these lava tubes formed at relatively low local flow rate, low lava viscosity, and sustained magma supply during a long period. Besides, lava flow inflation is also important in the formation of the ridge-like lava tubes and some associated features. These lava tubes provide efficient lateral pathways for magma transportation over the relatively low topographic slopes in southeast Tharsis, and they are important for the formation of long

lava flows in this region. The findings of this study provide an alternative formation mechanism for sinuous ridges on the martian surface.

Keywords: lava tube; sinuous ridge; volcanism; Tharsis; Mars

1. Introduction

Lava tubes are common volcanic features with linear or curvilinear, tunnel-like appearances. Lava tube systems are widely distributed in volcanic fields on Earth, e.g., Mount Etna in Italy (Calvari and Pinkerton, 1998), Kilauea Volcano in Hawaii (Peterson et al., 1994; Kauahikaua et al., 1998), and Undara Volcano in Australia (Atkinson et al., 1975; Stephenson et al., 1998). Besides Earth, lava tubes have been identified on other terrestrial planets and some natural satellites, e.g., Venus (Byrnes and Crown, 2002), the Earth's Moon (Greeley, 1971a; Coombs and Hawke, 1992), and Io (Crown et al., 1992; Keszthelyi et al., 2001). On Mars, lava tubes have been extensively identified with high-resolution imagery data (Keszthelyi et al., 2008; Léveillé and Datta, 2010; Leone, 2014). They are particularly concentrated on the flanks of big volcanoes in the Tharsis volcanic province, e.g., Alba Patera (Sakimoto et al., 1997; Ivanov and Head, 2006), Olympus Mons (Sakimoto et al., 1997; Bleacher et al., 2007a), and Tharsis Montes (Bleacher et al., 2007b; Xiao and Wang, 2009; Léveillé and Datta, 2010).

Lava tubes are important in the transportation of lavas and provide a window into the characteristics of volcanism, such as the magma composition, lava viscosity, effusion rate, and the duration of volcanic activity (Keszthelyi, 1995; Sakimoto et al., 1997; Kauahikaua et al., 1998). Lava tubes on the Moon and Mars would be ideal sites for the construction of human bases in planetary exploration, as they would protect people from solar radiation and small asteroid impacts, and provide a nearly constant temperature environment (Coombs and Hawke, 1992). In addition, they could serve as life shelters and are potential

sites for the search for extraterrestrial organisms (Léveillé and Datta, 2010). Therefore, identifying and studying lava tubes on planetary surfaces, including Mars, is important.

In this study, we identified 38 previously unreported sinuous ridges that have a lava-tube origin in southeast Tharsis (Fig. 1). Compared with previously identified planetary lava tubes, which are mostly indicated by skylights and discontinuous depressions, the ridge-like lava tubes identified in this study can be directly observed, and thus, their morphology and distribution are easier to be studied. We studied their geomorphology in detail using ~0.25 m/pixel images from High Resolution Imaging Science Experiment (HiRISE) (McEwen et al., 2007), ~6 m/pixel images from Context Camera (CTX) (Malin et al., 2007), ~100 m/pixel IR images and 19 m/pixel visible images from the Thermal Emission Imaging System (THEMIS) (Christensen et al., 2004), and 10–50 m/pixel images from the High Resolution Stereo Camera (HRSC) (Neukum and Jaumann, 2004). We used Mars Orbiter Laser Altimeter (MOLA) Mission Experiment Gridded Data Records (MEGDRs: ~462 m/pixel) to measure the regional topography and used MOLA Precision Experiment Data Records (PEDRs) where they were available to determine the relief of lava tubes. Digital terrain models (DTMs) generated from CTX stereopairs were also used to extract topographic profiles of lava tubes (Shean et al., 2011). In addition, we estimated their ages based on stratigraphic relationships and by performing crater size-frequency distribution measurements on their related features. We propose that these lava tube systems served as conduits for long-distance lava transportation and were important in the emplacement of long lava flows in the Tharsis plateau. The results of this study also provide an alternative formation mechanism of sinuous ridges on the Martian surface.

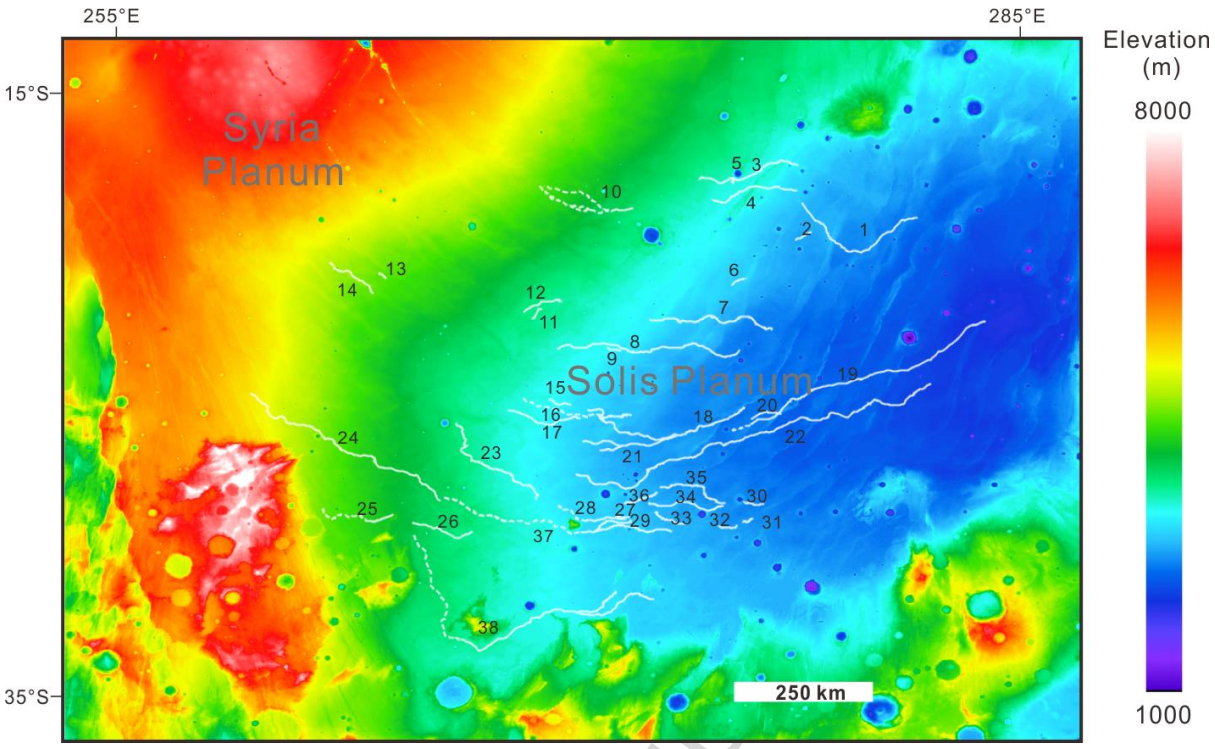

Fig. 1. Distribution of sinuous ridges (white solid lines) in southeast Tharsis. Numbers are the labels of the sinuous ridges listed in Table S1. White dashed lines indicate channels that are connected to the sinuous ridges. The background image is derived from MOLA MEGDRs (simple cylindrical projection).

2. Regional geology

Our study region is mainly located in the Solis Planum (Fig. 1), which is a large lava plain in the southeast Tharsis large volcanic province with rare evidence of surface modification by water or glaciers (Dohm and Tanaka, 1999; Huang and Xiao, 2014; Tanaka et al., 2014). This region spans 260–285°E longitude, 15–35°S latitude and covers an area of 1.2×10^6 km^2. The elevation decreases from more than 6000 m above Mars datum in the northwest to ~2000 m in the east (Fig. 1), and the regional slope decreases from ~0.5° to <0.1° from west to east. The study region is mainly comprised of two mapped geologic units: Early Hesperian volcanics (eHv) in the east and Late Hesperian volcanics (lHv) in the west (Tanaka et al., 2014). The eHv unit is characterized by lobate lava flows that are meters to tens of meters in thickness, and

eHv contains a number of wrinkle ridges that trend NNE-SSW and NE-SW. The lHv unit is also comprised of lobate flows but has fewer wrinkle ridges. The lobate lava flows in both units flowed from west to east and are as long as 1000 km.

3. Geomorphology of the sinuous ridges

3.1. Overall morphology

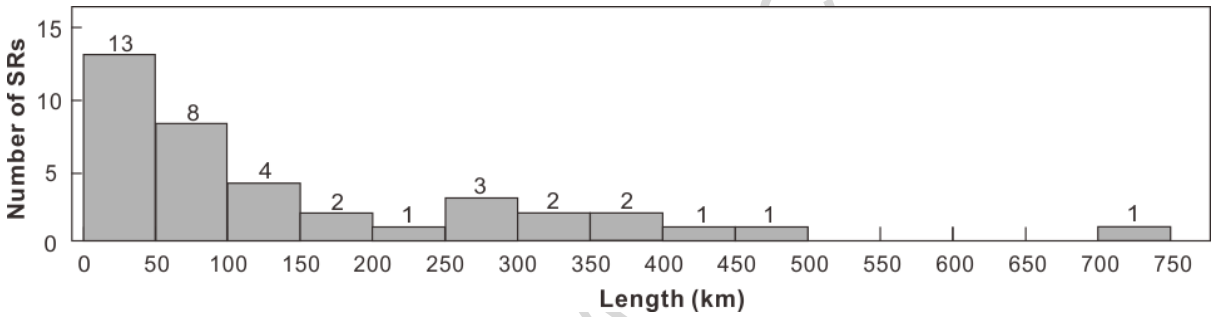

Fig. 2. Sinuous ridge (SR) length distribution histogram.

We identified 38 sinuous ridges (SRs) in southeast Tharsis (Fig. 1, Table S1). The lengths of the SRs vary between 14 and 743 km, with an average of 198 km and a standard deviation of 164 km. The length distribution histogram (Fig. 2) shows that about one-third of the SRs are <50 km in length, and SRs longer than 100 km are about 45% in number. The widths and heights of the SRs vary along their trending directions. The maximum width and height of the SRs can be up to 1.6 km and 20 m respectively. The trending direction of most SRs is NW-SE or W-E, which is consistent with the direction of lava flows in this region (Dohm and Tanaka, 1999; Tanaka et al., 2014). The slopes along these SRs are generally <0.3° and most of them are <0.1°. The head of most SRs are buried by younger lava flows (Fig. 3A) or ejecta from young craters (Fig. 3B). Eight of the 38 SRs are connected to channels in their upstream. The SR No. 25

(Fig. 4) is representative: a 350-m-wide channel is in the upper left of the image, and it transitions to an SR in the lower right. We have identified some unique streamlined islands in the channel (Fig. 4). In some cases, the transition from a channel to an SR is correlated with the change of slope, particularly for lengthy channels. For example, SR No. 37 is about 170 km long, and it is connected to a 230-km-long channel in its upstream (Fig. 5). The average slope along the channel is about 0.2°. The channel transitions to an SR when the elevation is <3300 m and the average slope along the SR is about 0.05°.

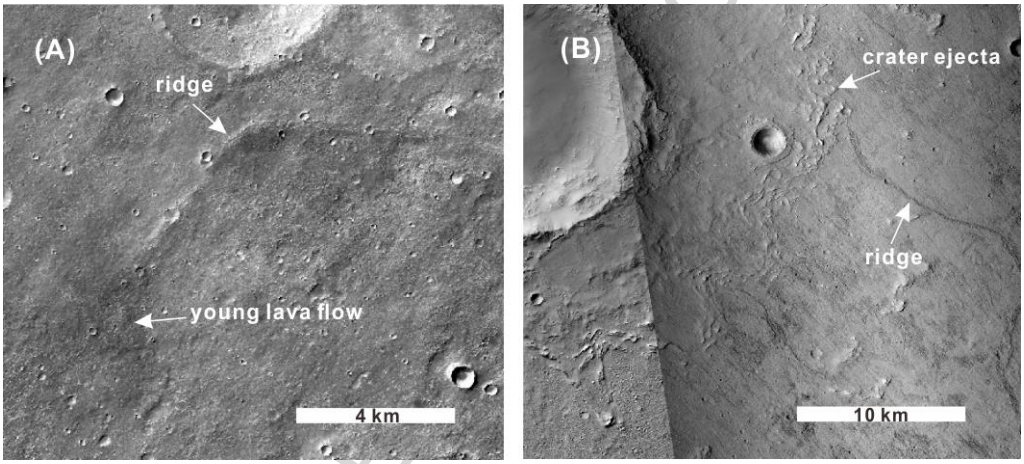

Fig. 3. Younger lava flows (**A**, SR No. 3 in Fig. 1; CTX: P21_009144_1621_XN_17S085W) or crater ejecta (**B**, SR No. 23 in Fig. 1; CTX: P12_005545_1515_XI_28S093W, G21_026326_1524_XN_27S094W) bury the heads of the sinuous ridges.

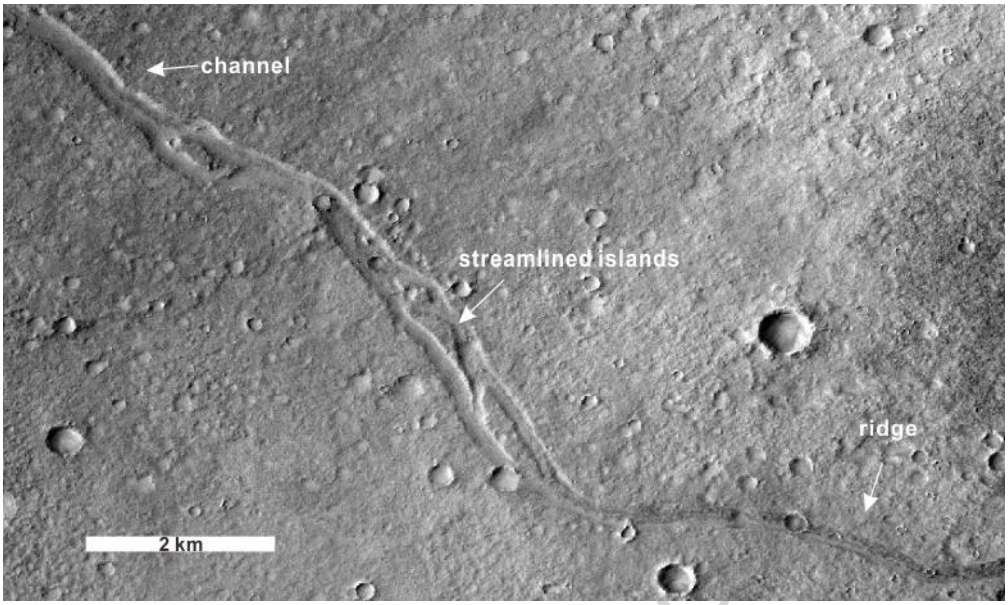

Fig. 4. Transition from a channel to a sinuous ridge (No. 25 in Fig. 1; CTX: F05_037574_1519_XN_28S096W). Streamlined islands can be observed.

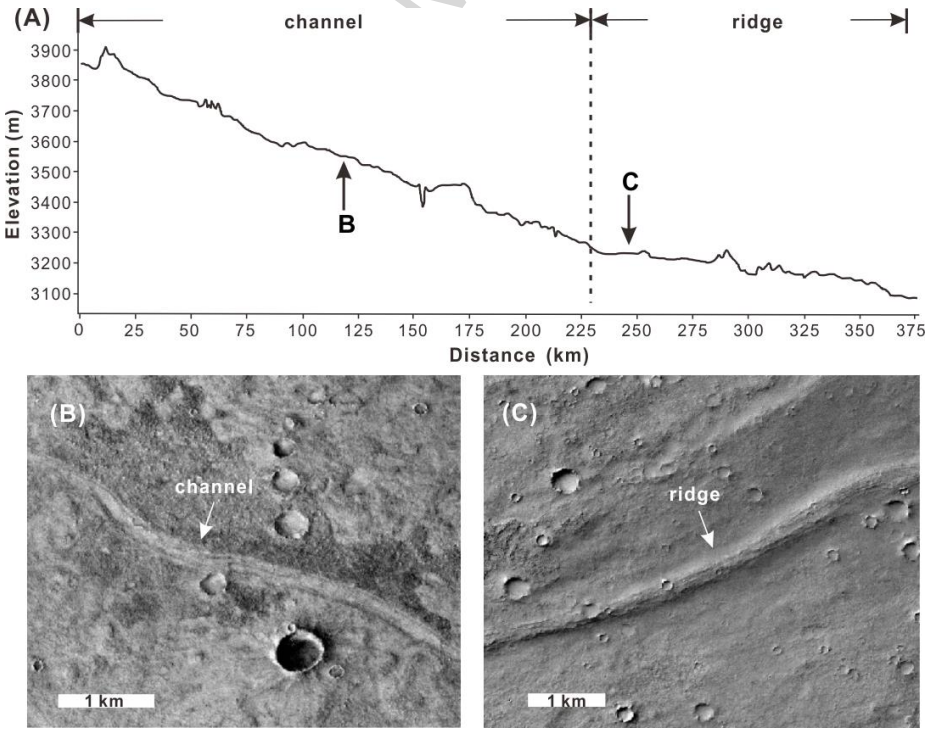

Fig. 5. Sinuous ridge No. 37 and the channel connected to it. (**A**) Elevation profile along its extension derived from MOLA data. (B) and (C) indicate the locations of the images in (B) and (C). (**B**) CTX image

of a part of the channel (CTX: D07_029860_1501_XN_29S091W). (**C**) CTX image of a part of the sinuous ridge (CTX: P19_008340_1510_XN_29S089W).

3.2. Cross-sectional shapes

The cross-sectional profiles of the SRs identified in this study are generally convex-upward with some local variations. The most common cross-sectional types are round-crested, double-ridged, and flat-crested (Fig. 6).

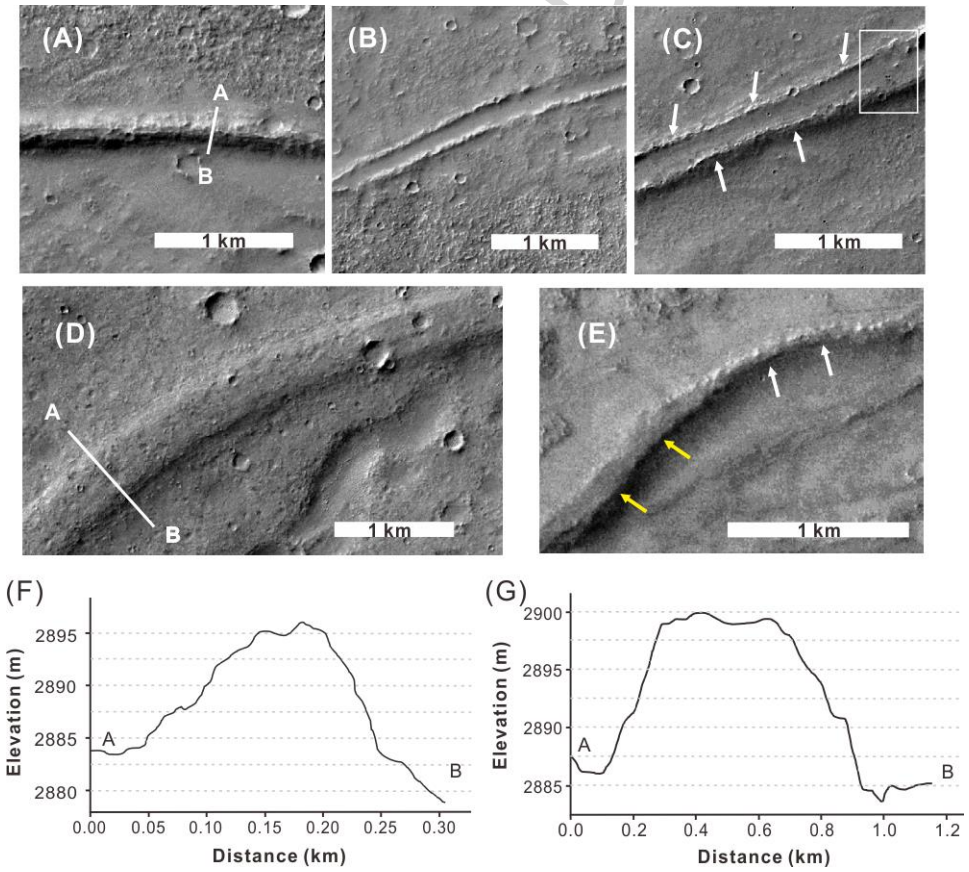

Fig. 6. Cross-sectional shapes of sinuous ridges (**A-E**) and two typical traverse elevation profiles (**F**, **G**). (**A**) round-crested (CTX: P19_008498_1529_XI_27S084W); (**B**) double-ridged (CTX: P20_008722_1542_XN_25S081W); (**C**) double-ridged, with two lateral ridges (indicated by arrows) on the

top of a high-standing broad ridge (CTX: P19_008366_1542_XI_25S080W). The area in the box shows the transformation from double-ridged shape to flat-crested shape resulting from the degradation of lateral ridges. (**D**) Flat-crested (CTX: D22_035925_1619_XN_18S079W); (**E**) transformation from flat-crested type (indicated by yellow arrows) to round-crested type (indicated by white arrows) (CTX: B04_011267_1527_XI_27S085W); (**F**) elevation profile along the line AB in (A), derived from CTX DTM; (**G**) elevation profile along the line AB in (D), derived from CTX DTM.

- Round-crested (Figs. 6A, 6F). This type of ridge has an arched cross-sectional shape. The width is between 0.1 and 1.1 km, while the height varies considerably. This is the most common profile type. An example of a round-crested type (Fig. 6A) has a width of ~0.3 km and height of ~15 m according to CTX DTM data.
- Double-ridged (Figs. 6B, 6C). This type is characterized by two parallel ridges with relatively flat terrain between them. The width of these ridges varies between 0.5 and 1.2 km. Some parallel ridges can occur on the top of a high-standing broad ridge and transition to lateral ridges (Fig. 6C). This type of ridge can protrude up to 15 m above the surrounding plains. A typical double-ridged type (Fig. 6C) has an average width of ~500 m and height of 8 m based on MOLA PEDRs. In addition, by measuring the shadow of the lateral ridge on the top of the broad ridge, we estimated that the height of lateral ridges is ~2 m.
- Flat-crested (Figs. 6D, 6G). This type has a broad and flat top, the width of which varies between 0.3 and 1.6 km. The height can be >10 m. A representative flat-crested type (Fig. 6D) has a width of ~900 m and a height of ~15 m, and the flank slope is ~5.3°.

In a single SR, different types of cross-sectional shapes can be observed and they can transform with each other. For example, in Fig. 5C, the cross section of the SR changes from double-ridged type to flat-crested type in the box; Fig. 5E shows the transformation from flat-crested to round-crested type.

3.3. Detailed features

3.3.1. Branches

We observed 13 SRs with branches. The branch angles range between 10 and 50°. Two types of branches were identified: the first type of branch is usually broad. It extends a short distance from the branch point, and in most cases two branches are seen to merge together again (Fig. 7A); the other type of branch is relatively narrow and can extend for a longer distance (Fig. 7B).

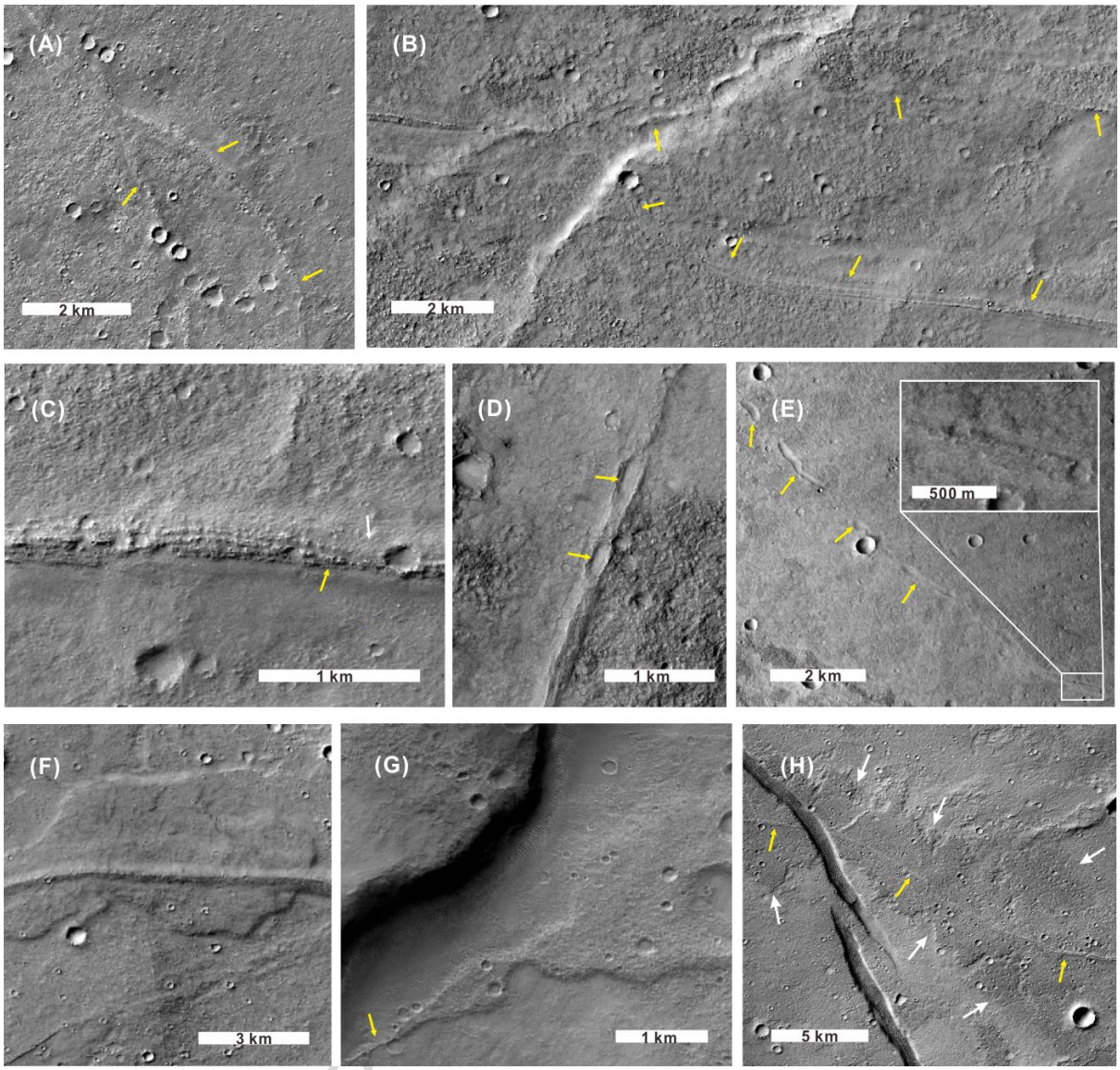

Fig. 7. Detailed features of the sinuous ridges. (**A**) A sinuous ridge with broad and short branches (arrows point to the two branches, CTX: P18_008076_1603_XI_19S081W); (**B**) a sinuous ridge with narrow and long branches (arrows point to the two branches, CTX: G20_026194_1483_XN_31S089W); (**C**) axial cracks on the top of a sinuous ridge (CTX: B20_017412_1462_XN_33S089W). They can merge together (pointed by the yellow arrow) or are covered by crater ejecta (white arrow); (**D**) discontinuous depressions on the top of a sinuous ridge (indicated by arrows; CTX: D14_032774_1583_XN_21S091W); (**E**) discontinuous depressions (indicated by arrows) that transform to a sinuous ridge (inset; CTX: D07_030005_1536_XN_26S090W); (**F**) lobate features (CTX: P20_008854_1522_XI_27S086W,

P19_008564_1519_XI_28S086W); (**G**) a delta-shaped feature at the end of a sinuous ridge (indicated by the arrow; CTX: P13_006138_1555_XN_24S084W); and (**H**) a lava flow associated with a sinuous ridge (indicated by white arrows; yellow arrows indicate the sinuous ridge; CTX: G20_026181_1498_XN_30S094W).

3.3.2. Axial cracks

In the study region, axial cracks usually present on the tops of SRs with round-crest cross-sectional shapes (Fig. 7C). They usually extend along the trending direction of SRs and can merge together or divide into sub-parallel en echelon segments. For example, in Fig. 7C, multiple axial cracks with a maximum width of ~40 m can be seen. They can extend more than a few kilometers, and some cracks merged together at the position pointed by yellow arrows in Fig. 7C. In some cases, they could be covered by crater ejecta or dust (indicated by white arrow in Fig. 7C).

3.3.3. Discontinuous depressions

Discontinuous depressions are typically elliptical in shape with the long axis trending in the direction of an SR. Most discontinuous depressions are found on the top of the SRs (Fig. 7D), but some discontinuous depressions occur in the adjacent lava plain and can gradually transform to SRs (Fig. 7E). An example of discontinuous, irregular depressions is shown in Fig. 7E. The width of depressions is about 250 m, and the longest depression is about 1.8 km in length. The depressions transform to a 300-m-wide SR southeast of the scene.

3.3.4. Lobate features

In the study region, most of the SRs exhibit lobate features along their trending direction (Fig. 7F). Lobes can be located on one side or both sides of an SR and are3 to 10 times the width of the SR. These lobate features usually have steep margins.

3.3.5. Delta-shaped features

Delta-shaped features occur in the middle or at the end of the SRs (Fig. 7G). In the study region, delta-shaped features can cover an area of 20 to 340 km^2. These estimates are lower limits as most delta-shaped features have been modified by subsequent geologic processes.

3.3.6. Associated lava flows

Some of the SRs are observed associated with lava flows. The SRs are usually located in the middle of lava flows and have same trending directions with the lava flows. Most of these lava flows are not well preserved owing to subsequent modification processes such as burial of younger lava flows. Besides, some associated lava flows are flat-topped, steep-sided, and usually occur in the middle or at the end of an SR. Fig. 7H shows a typical lava flow with an SR located within the middle of it. The lava flow extends in the same direction as the SR, and the width is up to 10 km.

4. Age determination

We constrained the formation time of the SRs using stratigraphic relationships. A total of 28 SRs occur in the Late Hesperian unit (lHv) or in the Late (lHv) and Early Hesperian units (eHv), while the rest are entirely in an Early Hesperian unit (eHv). This provides a lower age bound for the SRs, indicating that most SRs are formed in Late Hesperian. The upper age limit can be constrained by the relationship between the SRs and the wrinkle ridges. Nearly 30 SRs are intersected by wrinkle ridges that are formed mainly in Late

Hesperian (Mangold et al., 2000; Anderson et al., 2008). For instance, the SR No. 22 is intersected and partly destroyed by a wrinkle ridge (Fig. 8), which indicates that the SR is older than the wrinkle ridge. Therefore, these relationships indicate that most of the SRs formed in Late Hesperian.

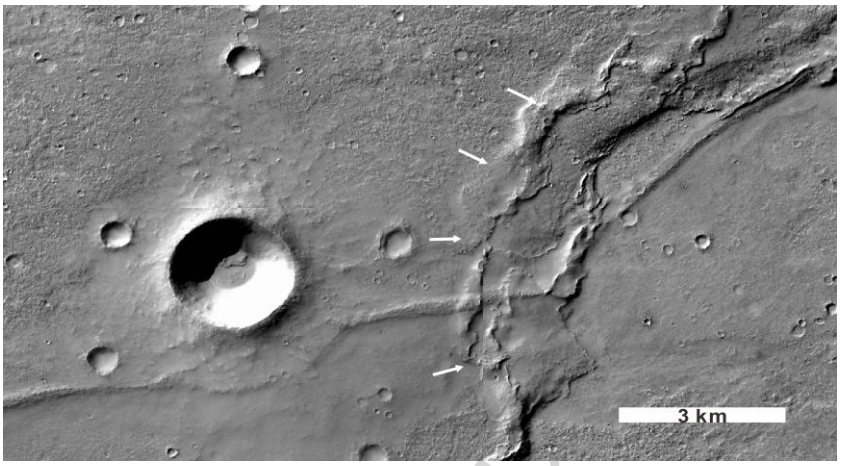

Fig. 8. A sinuous ridge that was intersected by wrinkle ridges (indicated by arrows), indicating an older age of the sinuous ridge (CTX: P19_008498_1529_XI_27S084W).

Some landforms such as lobate features, delta-shaped features, and lava flows have been found associated with the SRs (see section 3.3). The absolute model ages of these features can provide constraints on the active age of SRs. In this study, crater size-distribution measurements (Michael and Neukum, 2010) were performed to acquire their ages. We selected four areas that were less affected by later modification processes, such as wrinkle ridge formation or onlapping ejecta from large craters to perform crater counting. Then we used the software craterstats2 and chose the production function proposed by Ivanov (2001) and the chronology curve by Hartmann and Neukum (2001) to obtain the absolute model ages. The results (Table 1, Fig. 9) show that all four regions have ages of near the Hesperian-Amazonian boundary, which should be the active ages of the SRs. Taking dating results from

stratigraphic relationships into consideration, we can tell that the SRs formed mainly in Late Hesperian and are probably active until the Hesperian-Amazonian boundary.

Table 1

Dating results of the four studied regions

SR label	Crater counting area (km^2)	N(1) (km^{-2})	Absolute model age (Ga)
8	85.659	1.55×10^{-3}	3.07 (+0.15/-0.26)
18	18.217	1.51×10^{-3}	3.02 (+0.21/-0.41)
22	28.169	1.67×10^{-3}	3.18 (+0.17/-0.47)
24	159.356	1.59×10^{-3}	3.11 (+0.13/-0.24)

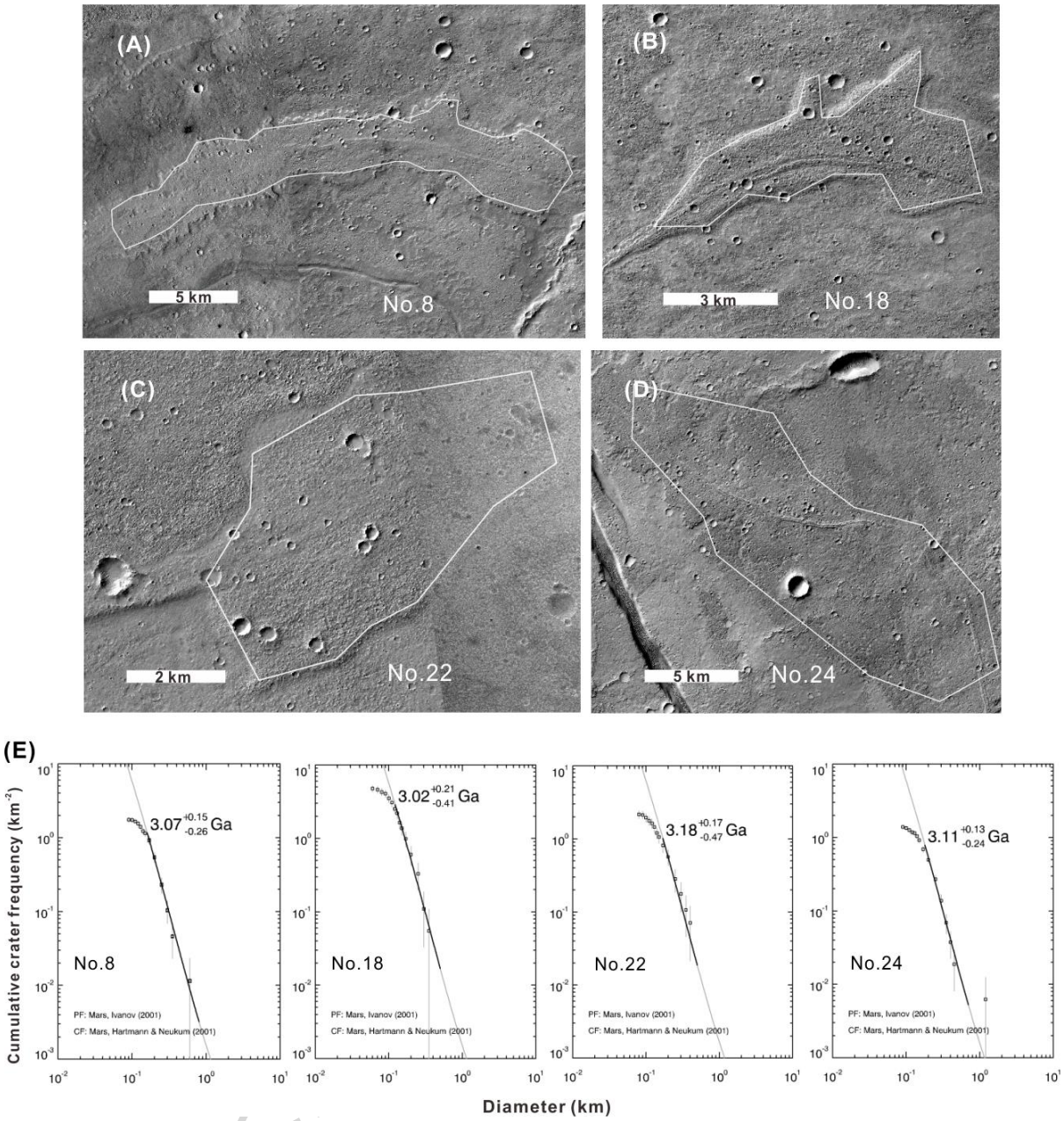

Fig. 9. Regions for crater counting (**A-D**, denoted by white lines) and the dating results of each region **(E)**.

CTX data IDs: (A) G09_021605_1567_XN_23S086W, P20_008999_1565_XI_23S085W; (B) B18_016713_1546_XN_25S086W; (C) P21_009091_1538_XN_26S077W, P11_005162_1546_XN_25S077W; (D) G20_026181_1498_XN_30S094W, B18_016832_1514_XN_28S094W.

5. Discussion

5.1. A lava-tube origin for the sinuous ridges in southeast Tharsis

Sinuous ridges are widely distributed on the Martian surface, most of which are concentrated in the Aeolis-Zephyria region (Burr et al., 2009; Williams et al., 2013), Hellas and Argyre basins (Kargel and Strom, 1992; Banks et al., 2009), Valles Marineris and nearby chasmata (Weitz et al., 2010), Arabia Terra (Davis et al., 2016), and the South Polar region (Head, 2000; Head and Pratt, 2001; Kress and Head, 2015). Several origins of SRs have been proposed, including surficial lava flows, wrinkle ridges, sinuous dunes, igneous dikes, inverted stream valleys, eskers, etc. (Head, 2000; Williams et al., 2013). Among them, igneous dike, inverted stream valley, and esker origins are the most popular hypotheses. We considered these hypotheses but found they cannot explain the SRs in southeast Tharsis.

Surficial lava flows are usually flat and broad with lobate margins (Theilig and Greeley, 1986), whereas the SRs are curvilinear, relatively narrow, diverse in their cross-sectional profiles, and usually have relatively regular and steep margins. Wrinkle ridges are elongated and sinuous positive landforms that usually consist of a broad and linear rise topped by a narrow and contorted ridge (Bryan, 1973). Wrinkle ridges have asymmetrical cross-sectional profiles. In contrast, SRs are usually symmetrical and have unique cross-sectional shapes (e.g., double-ridged) not exhibited by wrinkle ridges. From high-resolution images, we find that SRs usually have rocky surfaces. This and the lobate features related to some SRs are inconsistent with a dune hypothesis.

Igneous dikes have been identified in Thaumasia Planum (Huang et al., 2012). However, dikes are always less sinuous, have fewer branches, and have relatively uniform cross-sectional shapes. Moreover, channels with streamlined island features (Fig. 4) have been observed connected to some of the SRs, which

could not happen with dikes. In addition, dikes would not have delta-shaped features at their ends (Banks et al., 2009; Huang et al., 2012).

Most SRs on Mars have been considered as inverted valleys. An inverted valley forms when a channel undergoes a solidification process and the floor of the valley becomes more erosion-resistant than the adjacent terrains. After its surrounding materials are removed, the valley floor becomes an inverted valley (Pain et al., 2007). We ruled out the inverted valley origin because these SRs lack geomorphological features such as layers, oxbow lakes, and lake basins that are typically associated with inverted valleys. Besides, inverted valleys usually show dendritic planimetric pattern or branching networks, whereas the SRs are mostly single ridges with very few branches. Moreover, discontinuous depressions and lobate features identified with these SRs are rarely seen in inverted valleys.

Previous studies have proposed criteria for the identification of eskers, including high branch angles, sharp profiles, and traversing topographic divides (Kargel and Strom, 1992; Banks et al., 2009). However, these criteria are equivocal without the accompanying identification of other glacier landforms in the same region (Burr et al., 2009; Williams et al., 2013). Solis Planum lacks glacial landforms, indicating that the SRs in this study are not eskers. Also, the discontinuous depressions identified here are rarely observed in eskers. Furthermore, the SRs generally follow the topographic gradient, which is more consistent with flowing lava than eskers.

After excluding the above hypotheses, we propose a lava-tube origin for the SRs in southeast Tharsis. Southeast Tharsis is a large lava plain that is covered by lava flows of several to hundreds of kilometers long and tens of meters thick (Simon et al., 2014). Fluvial and glacial landforms and aqueous minerals are rarely identified in previous studies (Dohm and Tanaka, 1999; Carter et al., 2013; Tanaka et al., 2014). This geologic setting suggests a volcanic origin for the SRs identified in this study. The curvilinear morphology

of the SRs and the associated landforms are all consistent with the lava tube origin. Some of the SRs extend into the middle of lava flows, and lava deltas are also found in the middle or at the end of some SRs. These lava flows and lava deltas could be formed by tube-fed lava. Similar tube-fed lava deltas have been observed in other regions on Mars and on the surface of Venus, and they represent local outpourings of lava from the lava flow within a tube (Byrnes and Crown, 2002; Bleacher et al., 2007a). Some flat-topped, steep-sided lava flows associated with the SRs could be sinuous plateaus described by Crown and Ramsey (2016) that is formed by lava inflation (Crown and Ramsey, 2016; Bleacher et al., 2017). Irregular pit chains or elongate depressions and uncollapsed segments observed along the SRs are also important indications of lava tubes. These features could be skylights that formed from roof collapse of a lava tube (Coombs and Hawke, 1992). The lobate features are actually breakouts from the lava tube walls and sinuous tumuli flanks because of pressurization in lava tubes (Orr et al., 2015). Similar breakout lobes have been identified near Tharsis Montes (Orr et al., 2015; Crown and Ramsey, 2016; Bleacher et al., 2017). Axial cracks are common features developed on the crest of sinuous tumuli and usually formed by lava pressure-driven inflationary events or thermal contraction during the cooling of lava (Walker, 1991; Calvari and Pinkerton, 1999; Kattenhorn and Schaefer, 2008; Orr et al., 2015). They will widen and deepen as inflation progressed and tumulus evolved (Orr et al., 2015). Streamlined islands are usually formed by liquid water; however, they could also be formed by low-viscosity lava (Leverington, 2004), and the streamlined islands identified in this study (Fig. 4) are features of volcanic origin according to the geologic context and other associated volcanic features. Besides, the SRs roughly trend along the elevation gradient and transition from a channel to an SR when the slope becomes gentle and/or the elevation decreases, also indicating a lava tube origin as lava channels form in preference over tubes when the slope

is steep and lava flows relatively fast (Greeley, 1971a). With the decrease of slope, lava flow rate slows, and lava tubes could form from roofing of lava channels.

In conclusion, the lava tube origin is the most reasonable formation mechanism for the SRs in southeast Tharsis. This result also indicates that more attention should be paid on the geologic background and associated features when we discuss the origin of Martian SRs.

5.2. Formation mechanism of the ridge-like cross-sectional shapes of the lava tubes

Lava tubes generally form in pahoehoe lava flows, although they have also been observed in ‘a‘a lava flows (Calvari and Pinkerton, 1998). Two main formation mechanisms of lava tubes have been proposed. The first is roofing of lava channels. An open lava channel can form a roof by growth of rooted crusts, piling up of lava crust pieces or levee overgrowth (Greeley, 1971b; Peterson et al., 1994). The other formation process involves the inflation of pahoehoe lava flows. Pahoehoe flows can develop a crust owing to cooling of its outermost portion while the lava beneath the crust remains fluid. This crust thickens and forms a solid roof above the flowing lava. As the interior flow advances and expands, complex tube systems can form (Hon et al., 1994; Peterson et al., 1994).

In most cases, the surface topographic relief is not obvious when a lava tube forms. However, two processes can lead to the formation of ridge-like lava tubes. The first process is levee accretion when the level of the lava stream fluctuates frequently (Peterson et al., 1994). This will lead to the formation of a convex-upward tube roof when the levees grow together. The second process is the formation of sinuous tumuli over an active lava tube, which results from lava inflation (Orr et al., 2015). In this situation, a sinuous tumulus tends to be more elongate and could exhibit a sinuous-ridge-like landform over the lava

tube. Orr et al. (2015) made a detailed survey of the formation of sinuous tumuli during the eruption of Kīlauea Volcano in Hawaii and suggested that an SR near Tharsis Montes could be its Martian counterpart. These processes lead to the formation of ridge-like profiles of the lava tubes in this study.

In addition, variations on the cross-sectional shapes of the lava tubes have also been observed. Among the three types of cross-sectional shapes, the round-crested type is most common. This type could be the original shape of ridge-like lava tubes, especially those with axial cracks that are indicators of sinuous tumuli on their crest. The round-crested type could also evolve from the flat-crested type owing to the degradation of the flanks, which has been shown in Fig. 6E. The double-ridged type would have formed when the roof of a lava tube collapsed but the tube walls remain standing. If the floor of the lava tube has similar elevation with the surrounding plain, a typical double-ridged profile as shown in Fig. 6B will form. In contrast, if the lava tube floor is higher than the surroundings, the remnant walls could become the lateral ridges (Fig. 6C). An example is shown in Fig. 7D in which the collapsed part of the lava tube has a double-ridged cross-sectional shape. The flat-crested type would have been transformed from double-ridged type when the lateral ridges degraded. An example of this transition is shown in the box region of Fig. 6C. In addition, lava channel roofing is also a possible formation mechanism for the flat-crested type.

5.3. Implications for Tharsis volcanism

Extensive magma emplacement occurred in the Syria-Thaumasia Block lava plains during the Hesperian (Dohm and Tanaka, 1999; Huang and Xiao, 2014; Tanaka et al., 2014). Understanding how these vast amounts of lava were transported and emplaced is important. While direct (Huang et al., 2012) and indirect (Wilson and Head, 2002) evidence of dikes indicate a pathway for the vertical transportation of magma in this region, the lava tube systems mapped in this study could be an efficient means for the horizontal

transportation of magma. Lava tubes can provide an insulated environment to keep lava warm and fluid (Greeley, 1987; Keszthelyi, 1995; Sakimoto and Zuber, 1998). Keszthelyi (1995) constructed the thermal budget for lava tubes and observed only 1℃/km cooling of the lava inside the active tube, which is important for the long distance transportation of lava. Therefore, lava tubes play key roles in the formation of long lava flows (Keszthelyi and Self, 1998; Stephenson et al., 1998; Zimbelman, 1998). A terrestrial example is North Queensland volcanic field in Australia where a number of long lava flows with lengths from 50 to 160 km emplaced on very low slopes of <0.5°. Lava tubes were extensively observed in this area and were considered to have fed the long lava flows (Stephenson et al., 1998). In our study region, the lava tubes identified are as long as 700 km and are mainly formed in the areas with average slopes <0.3°. They have the same trending direction as the lava flows, and evidence of tube-fed lava flows have been found. Therefore, these lava tubes could also play key roles in the emplacement of long lava flows (up to 1000 km) in southeast Tharsis.

Ridge-like lava tubes have also been identified in adjacent regions on the Tharsis plateau. Crown and Ramsey (2016) found SRs extend onto dark, smooth lava flows in southwestern Arsia Mons. Bleacher et al. (2017) also identified 163 SR segments in the east of Pavonis Mons. The SRs are up to 100 km in length and tens of meters in height. Both studies have observed breakout lobes and flat-topped sinuous plateaus associated with the SRs. These features could be formed by lava inflation and suggest relatively low local flow rate and low lava viscosity (Rowland and Walker, 1990; Hon et al., 1994; Crown and Baloga, 1999; Crown and Ramsey, 2016; Bleacher et al., 2017). In comparison, the SRs identified in our study have similar morphologic features and associated landforms (e.g., breakout lobes, sinuous plateaus), indicating the same origin that is related to lava inflation. Therefore, low flow rate and low lava viscosity are also needed in the formation of the SRs in southeast Tharsis. However, these SRs are larger in scale, with >40%

of the SRs longer than 100 km with a maximum of 743 km. We attribute this to a sustained magma supply and a longer active period of volcanic activity in the Syria-Thaumasia region, which have also been considered as important factors in the formation of long lava flows on Earth, e.g., the Carrizozo tube-fed lava flow in New Mexico (Keszthelyi and Pieri, 1993). Besides, the vast area and the gradually changing gradients of Syria and Solis Planum are also beneficial to the formation of these long SRs.

A problem existing in previous studies is that the lack of cracks or inflation clefts is not consistent with an inflation origin of Martian SRs (Garry et al., 2012; Orr et al., 2015; Bleacher et al., 2017). Bleacher et al. (2017) proposed a possible explanation that the cracks or clefts could be covered or filled by dust and therefore may not be detectable remotely. In this study, axial cracks have been recognized on the crest of some ridge-like lava tubes (Fig. 7C). This finding bridges the above problem and provides compelling evidence for the inflation origin of the ridge-like cross-sectional shape of the lava tubes. Besides, signatures of dust filling or crater ejecta covering on the axial cracks were also observed in this study, which may support the explanation proposed by Bleacher et al. (2017).

6. Conclusions

We identified 38 ridge-like lava tubes in southeast Tharsis and analyzed their morphology and ages. Most of the lava tubes should form in Late Hesperian and are active until the Hesperian-Amazonian boundary. Their ridge-like cross-sectional shape and some associated features such as breakout lobes and axial cracks are related to lava flow inflation. Low flow rate, low lava viscosity, and sustained magma supply could be the main factors in the formation of the long lava tubes. These lava tubes could serve as lateral pathways for magma transportation over the relatively low topographic slopes and play an important role in the formation of long lava flows in southeast Tharsis. The lava tubes identified here indicate that

portions of sinuous ridges on Mars are of lava-tube origin and that they provide a window to lava properties and eruption conditions on Mars.

Acknowledgements

This study was supported by the National Scientific Foundation of China [No. 41403052; No. 41403056], the Fundamental Research Funds for National University, China University of Geosciences (Wuhan), and Key Laboratory of Planetary Sciences of CAS [PSL15_05]. Data can be accessed from JMARS (jmars.asu.edu) and PDS (pds.jpl.nasa.gov) with IDs. We are grateful to the editor and two anonymous reviewers for their comments and suggestions that greatly improved our manuscript.

References

Anderson, R.C., Dohm, J.M., Haldemann, A.F.C., Pounders, E., Golombek, M., Castano, A., 2008. Centers of tectonic activity in the eastern hemisphere of Mars. Icarus 195, 537-546. http://dx.doi.org/10.1016/j.icarus.2007.12.027.

Atkinson, A., Griffin, T.J., Stephenson, P.J., 1975. A major lava tube system from Undara Volcano, North Queensland. Bull. Volcanol. 39, 266-293. http://dx.doi.org/10.1007/bf02597832.

Banks, M.E., Lang, N.P., Kargel, J.S., McEwen, A.S., Baker, V.R., Grant, J.A., Pelletier, J.D., Strom, R.G., 2009. An analysis of sinuous ridges in the southern Argyre Planitia, Mars using HiRISE and CTX images and MOLA data. J. Geophys. Res. 114, E09003. http://dx.doi.org/10.1029/2008je003244.

Bleacher, J.E., Greeley, R., Williams, D.A., Cave, S.R., Neukum, G., 2007a. Trends in effusive style at the Tharsis Montes, Mars, and implications for the development of the Tharsis province. J. Geophys. Res. 112, E09005. http://dx.doi.org/10.1029/2006je002873.

Bleacher, J.E., Greeley, R., Williams, D.A., Werner, S.C., Hauber, E., Neukum, G., 2007b. Olympus Mons, Mars: Inferred changes in late Amazonian aged effusive activity from lava flow mapping of Mars Express High Resolution Stereo Camera data. J. Geophys. Res. 112, E04003. http://dx.doi.org/10.1029/2006je002826.

Bleacher, J.E., Orr, T.R., de Wet, A.P., Zimbelman, J.R., Hamilton, C.W., Brent Garry, W., Crumpler, L.S., Williams, D.A., 2017. Plateaus and sinuous ridges as the fingerprints of lava flow inflation in the Eastern Tharsis Plains of Mars. J. Volcanol. Geotherm. Res., in press. http://dx.doi.org/10.1016/j.jvolgeores.2017.03.025.

Bryan, W.B., 1973. Wrinkle-ridges as deformed surface crust on ponded mare lava. Geochim. Cosmochim. ac. suppl. 4, 93-106.

Burr, D.M., Enga, M.-T., Williams, R.M.E., Zimbelman, J.R., Howard, A.D., Brennand, T.A., 2009. Pervasive aqueous paleoflow features in the Aeolis/Zephyria Plana region, Mars. Icarus 200, 52-76. http://dx.doi.org/10.1016/j.icarus.2008.10.014.

Byrnes, J.M., Crown, D.A., 2002. Morphology, stratigraphy, and surface roughness properties of Venusian lava flow fields. J. Geophys. Res. 107, 9-1-9-22. http://dx.doi.org/10.1029/2001je001828.

Calvari, S., Pinkerton, H., 1998. Formation of lava tubes and extensive flow field during the 1991-1993 eruption of Mount Etna. J. Geophys. Res. 103, 27291-27301. http://dx.doi.org/10.1029/97jb03388.

Calvari, S., Pinkerton, H., 1999. Lava tube morphology on Etna and evidence for lava flow emplacement

mechanisms. J. Volcanol. Geotherm. Res. 90(3-4), 263-280. http://dx.doi.org/10.1016/s0377-0273(99)00024-4.

Carter, J., Poulet, F., Bibring, J.P., Mangold, N., Murchie, S., 2013. Hydrous minerals on Mars as seen by the CRISM and OMEGA imaging spectrometers: Updated global view. J. Geophys. Res. 118(4), 831-858. http://dx.doi.org/10.1029/2012je004145.

Christensen, P.R., Jakosky, B.M., Kieffer, H.H., Malin, M.C., McSween Jr, H.Y., Nealson, K., Mehall, G.L., Silverman, S.H., Ferry, S., Caplinger, M., 2004. The thermal emission imaging system (THEMIS) for the Mars 2001 Odyssey Mission. Space Sci. Rev. 110, 85-130. http://dx.doi.org/10.1023/B:SPAC.0000021008.16305.94.

Coombs, C.R., Hawke, B., 1992. A Search for Intact Lava Tubes on the Moon: Possible Lunar Base Habitats. In: Mendell, W.W. (Ed.), The Second Conference on Lunar Bases and Space Activities of the 21st Century. Lunar and Planetary Institute, Houston, TX, pp. 219–229.

Crown, D.A., Baloga, S.M., 1999. Pahoehoe toe dimensions, morphology, and branching relationships at Mauna Ulu, Kilauea Volcano, Hawai'i. Bull. Volcanol. 61(5), 288-305. http://dx.doi.org/10.1007/s004450050298.

Crown, D.A., Ramsey, M.S., 2016. Morphologic and thermophysical characteristics of lava flows southwest of Arsia Mons, Mars. J. Volcanol. Geotherm. Res., in press. http://dx.doi.org/10.1016/j.jvolgeores.2016.07.008.

Crown, D.A., Greeley, R., Craddock, R.A., Schaber, G.G., 1992. Geologic map of Io. USGS Misc. Investigations Series Map I-2209.

Davis, J., Balme, M., Grindrod, P., Williams, R., Gupta, S., 2016. Extensive Noachian fluvial systems in Arabia Terra: Implications for early Martian climate. Geology 44(10), 847-850.

http://dx.doi.org/10.1130/G38247.1.

Dohm, J.M., Tanaka, K.L., 1999. Geology of the Thaumasia region, Mars: plateau development, valley origins, and magmatic evolution. Planet. Space Sci. 47, 411-431. http://dx.doi.org/10.1016/s0032-0633(98)00141-x.

Garry, W., Robinson, M., Zimbelman, J., Bleacher, J., Hawke, B., Crumpler, L., Braden, S., Sato, H., 2012. The origin of Ina: Evidence for inflated lava flows on the Moon. J. Geophys. Res. 117(E12), E00H31. http://dx.doi.org/10.1029/2011JE003981

Greeley, R., 1971a. Lava tubes and channels in the lunar Marius Hills. The Moon 3, 289-314. http://dx.doi.org/10.1007/bf00561842.

Greeley, R., 1971b. Observations of actively forming lava tubes and associated structures. Mod. Geol. 2, 207-223.

Greeley, R., 1987. The role of lava tubes in Hawaiian volcanoes. US Geol. Surv. Prof. Pap 1350(2), 1589-1602.

Hartmann, W.K., Neukum, G., 2001. Cratering chronology and the evolution of Mars. Space Sci. Rev. 96, 165-194. http://dx.doi.org/10.1007/978-94-017-1035-0_6.

Head, J.W., 2000. Tests for ancient polar deposits on Mars: Origin of esker-like sinuous ridges (Dorsa Argentea) using MOLA data. Lunar and Planetary Science Conference Abstracts, 1116.

Head, J.W., Pratt, S., 2001. Extensive Hesperian-aged south polar ice sheet on Mars: Evidence for massive melting and retreat, and lateral flow and ponding of meltwater. J. Geophys. Res. 106, 12275. http://dx.doi.org/10.1029/2000je001359.

Hon, K.E.N., Kauahikaua, J.I.M., Denlinger, R., Mackay, K., 1994. Emplacement and inflation of pahoehoe sheet flows: Observations and measurements of active lava flows on Kilauea Volcano,

Hawaii. Geol. Soc. Am. Bull. 106, 351-370. http://dx.doi.org/10.1130/0016-7606(1994)106<0351:eaiops>2.3.co;2.

Huang, J., Xiao, L., 2014. Compositional evolution of lava plains in the Syria-Thaumasia Block, Mars. Sci. China, Phys. Mech. Astron. 57, 994-1000. http://dx.doi.org/10.1007/s11433-014-5407-3.

Huang, J., Edwards, C.S., Horgan, B.H.N., Christensen, P.R., Kraft, M.D., Xiao, L., 2012. Identification and mapping of dikes with relatively primitive compositions in Thaumasia Planum on Mars: Implications for Tharsis volcanism and the opening of Valles Marineris. Geophys. Res. Lett. 39, L17201. http://dx.doi.org/10.1029/2012gl052523.

Ivanov, B.A., 2001. Mars/Moon Cratering Rate Ratio Estimates. Space Sci. Rev. 96, 87-104. http://dx.doi.org/10.1007/978-94-017-1035-0_4.

Ivanov, M.A., Head, J.W., 2006. Alba Patera, Mars: Topography, structure, and evolution of a unique late Hesperian–early Amazonian shield volcano. J. Geophys. Res. 111, E09003. http://dx.doi.org/10.1029/2005je002469.

Kargel, J.S., Strom, R.G., 1992. Ancient glaciation on Mars. Geology 20, 3-7. http://dx.doi.org/10.1130/0091-7613(1992)020<0003:AGOM>2.3.CO;2.

Kattenhorn, S.A., Schaefer, C.J., 2008. Thermal–mechanical modeling of cooling history and fracture development in inflationary basalt lava flows. J. Volcanol. Geotherm. Res. 170(3-4), 181-197. http://dx.doi.org/10.1016/j.jvolgeores.2007.10.002.

Kauahikaua, J., Cashman, K.V., Mattox, T.N., Heliker, C.C., Hon, K.A., Mangan, M.T., Thornber, C.R., 1998. Observations on basaltic lava streams in tubes from Kilauea Volcano, island of Hawai'i. J. Geophys. Res. 103, 27303. http://dx.doi.org/10.1029/97jb03576.

Keszthelyi, L., 1995. A preliminary thermal budget for lava tubes on the Earth and planets. J. Geophys.

Res. 100, 20411-20420. http://dx.doi.org/10.1029/95jb01965.

Keszthelyi, L.P., Pieri, D.C., 1993. Emplacement of the 75-km-long Carrizozo lava flow field, south-central New Mexico. J. Volcanol. Geotherm. Res. 59(1), 59-75. http://dx.doi.org/10.1016/0377-0273(93)90078-6

Keszthelyi, L., Self, S., 1998. Some physical requirements for the emplacement of long basaltic lava flows. J. Geophys. Res. 103(B11), 27447-27464. http://dx.doi.org/10.1029/98jb00606.

Keszthelyi, L., McEwen, A.S., Phillips, C.B., Milazzo, M., Geissler, P., Turtle, E.P., Radebaugh, J., Williams, D.A., Simonelli, D.P., Breneman, H.H., Klaasen, K.P., Levanas, G., Denk, T., 2001. Imaging of volcanic activity on Jupiter's moon Io by Galileo during the Galileo Europa Mission and the Galileo Millennium Mission. J. Geophys. Res. 106, 33025-33052. http://dx.doi.org/10.1029/2000je001383.

Keszthelyi, L., Jaeger, W., McEwen, A., Tornabene, L., Beyer, R.A., Dundas, C., Milazzo, M., 2008. High Resolution Imaging Science Experiment (HiRISE) images of volcanic terrains from the first 6 months of the Mars Reconnaissance Orbiter Primary Science Phase. J. Geophys. Res. 113, E04005. http://dx.doi.org/10.1029/2007je002968.

Kress, A.M., Head, J.W., 2015. Late Noachian and early Hesperian ridge systems in the south circumpolar Dorsa Argentea Formation, Mars: Evidence for two stages of melting of an extensive late Noachian ice sheet. Planet. Space Sci. 109-110, 1-20. http://dx.doi.org/10.1016/j.pss.2014.11.025.

Leone, G., 2014. A network of lava tubes as the origin of Labyrinthus Noctis and Valles Marineris on Mars. J. Volcanol. Geotherm. Res. 277, 1-8. http://dx.doi.org/10.1016/j.jvolgeores.2014.01.011.

Léveillé, R.J., Datta, S., 2010. Lava tubes and basaltic caves as astrobiological targets on Earth and Mars: a

review. Planet. Space Sci. 58, 592-598. http://dx.doi.org/10.1016/j.pss.2009.06.004.

Leverington, D.W., 2004. Volcanic rilles, streamlined islands, and the origin of outflow channels on Mars. J. Geophys. Res. 109, E10011. http://dx.doi.org/10.1029/2004je002311.

Malin, M.C., Bell, J.F., Cantor, B.A., Caplinger, M.A., Calvin, W.M., Clancy, R.T., Edgett, K.S., Edwards, L., Haberle, R.M., James, P.B., Lee, S.W., Ravine, M.A., Thomas, P.C., Wolff, M.J., 2007. Context Camera Investigation on board the Mars Reconnaissance Orbiter. J. Geophys. Res. 112, E05S04. http://dx.doi.org/10.1029/2006je002808.

Mangold, N., Allemand, P., Thomas, P., Vidal, G., 2000. Chronology of compressional deformation on Mars: Evidence for a single and global origin. Planet. Space Sci. 48, 1201-1211. http://dx.doi.org/10.1016/S0032-0633(00)00104-5.

McEwen, A.S., Eliason, E.M., Bergstrom, J.W., Bridges, N.T., Hansen, C.J., Delamere, W.A., Grant, J.A., Gulick, V.C., Herkenhoff, K.E., Keszthelyi, L., Kirk, R.L., Mellon, M.T., Squyres, S.W., Thomas, N., Weitz, C.M., 2007. Mars Reconnaissance Orbiter's High Resolution Imaging Science Experiment (HiRISE). J. Geophys. Res. 112, E05S02. http://dx.doi.org/10.1029/2005je002605.

Michael, G.G., Neukum, G., 2010. Planetary surface dating from crater size–frequency distribution measurements: Partial resurfacing events and statistical age uncertainty. Earth Planet. Sci. Lett. 294, 223-229. http://dx.doi.org/10.1016/j.epsl.2009.12.041.

Neukum, G., Jaumann, R., 2004. HRSC: the High Resolution Stereo Camera of Mars Express. In: Wilson, A. (Ed.), Mars Express: The Scientific Payload. Eur. Space Agency Spec. Publ., ESA-SP, vol. 1240, pp. 17–35.

Orr, T.R., Bleacher, J.E., Patrick, M.R., Wooten, K.M., 2015. A sinuous tumulus over an active lava tube at Kīlauea Volcano: Evolution, analogs, and hazard forecasts. J. Volcanol. Geotherm. Res. 291,

35-48. http://dx.doi.org/10.1016/j.jvolgeores.2014.12.002.

Pain, C., Clarke, J., Thomas, M., 2007. Inversion of relief on Mars. Icarus 190, 478-491. http://dx.doi.org/10.1016/j.icarus.2007.03.017.

Peterson, D.W., Holcomb, R.T., Tilling, R.I., Christiansen, R.L., 1994. Development of lava tubes in the light of observations at Mauna Ulu, Kilauea Volcano, Hawaii. Bull. Volcanol. 56, 343-360. http://dx.doi.org/10.1007/BF00326461.

Rowland, S.K., Walker, G.P., 1990. Pahoehoe and aa in Hawaii: volumetric flow rate controls the lava structure. Bull. Volcanol. 52(8), 615-628. http://dx.doi.org/10.1007/BF00301212

Sakimoto, S.E.H., Zuber, M.T., 1998. Flow and convective cooling in lava tubes. J. Geophys. Res. 103(B11), 27465-27487. http://dx.doi.org/10.1029/97jb03108.

Sakimoto, S.E.H., Crisp, J., Baloga, S.M., 1997. Eruption constraints on tube-fed planetary lava flows. J. Geophys. Res. 102, 6597. http://dx.doi.org/10.1029/97je00069.

Shean, D., Fahle, J., Malin, M., Edwards, L., Posiolova, L., 2011. MRO CTX stereo image processing and preliminary DEM quality assessment. Lunar and Planetary Science Conference Abstracts, 2646.

Simon, M.N., Carter, L.M., Campbell, B.A., Phillips, R.J., Mattei, S., 2014. Studies of lava flows in the Tharsis region of Mars using SHARAD. J. Geophys. Res. 119(11), 2291-2299. doi: 10.1002/2014je004666.

Stephenson, P.J., Burch-Johnston, A.T., Stanton, D., Whitehead, P.W., 1998. Three long lava flows in north Queensland. J. Geophys. Res. 103, 27359-27370. http://dx.doi.org/10.1029/98jb01670.

Tanaka, K.L., Skinner Jr, J.A., Dohm, J.M., Irwin III, R.P., Kolb, E.J., Fortezzo, C.M., Platz, T., Michael, G.G., Hare, T.M., 2014. Geologic map of Mars. USGS. Sci. Invest. Map 3292.

Theilig, E., Greeley, R., 1986. Lava flows on Mars: Analysis of small surface features and comparisons

with terrestrial analogs. J. Geophys. Res. 91, E193-E206. http://dx.doi.org/10.1029/JB091iB13p0E193.

Walker, G.P., 1991. Structure, and origin by injection of lava under surface crust, of tumuli,"lava rises","lava-rise pits", and "lava-inflation clefts" in Hawaii. Bull. Volcanol. 53(7), 546-558. http://dx.doi.org/10.1007/BF00298155.

Weitz, C.M., Milliken, R.E., Grant, J.A., McEwen, A.S., Williams, R.M.E., Bishop, J.L., Thomson, B.J., 2010. Mars Reconnaissance Orbiter observations of light-toned layered deposits and associated fluvial landforms on the plateaus adjacent to Valles Marineris. Icarus 205, 73-102. http://dx.doi.org/10.1016/j.icarus.2009.04.017.

Williams, R.M.E., Irwin, R.P., Burr, D.M., Harrison, T., McClelland, P., 2013. Variability in martian sinuous ridge form: Case study of Aeolis Serpens in the Aeolis Dorsa, Mars, and insight from the Mirackina paleoriver, South Australia. Icarus 225, 308-324. http://dx.doi.org/10.1016/j.icarus.2013.03.016.

Wilson, L., Head, J.W., 2002. Tharsis‐radial graben systems as the surface manifestation of plume‐related dike intrusion complexes: Models and implications. J. Geophys. Res. 107, 1-1-1-24. http://dx.doi.org/10.1029/2001JE001593.

Xiao, L., Wang, C., 2009. Geologic features of Wudalianchi volcanic field, northeastern China: Implications for Martian volcanology. Planet. Space Sci. 57, 685-698. http://dx.doi.org/10.1016/j.pss.2008.08.005.

Zimbelman, J.R., 1998. Emplacement of long lava flows on planetary surfaces. J. Geophys. Res. 103(B11), 27503. http://dx.doi.org/10.1029/98jb01123.

Highlights

- 38 ridge-like lava tubes are identified in southeast Tharsis for the first time.
- Lava flow inflation is important in the formation of ridge-like lava tubes.
- Some of the widely distributed sinuous ridges on Mars are of lava-tube origin.
- Lava tubes play key roles in the formation of long lava flows in southeast Tharsis.